

Linear Model Predictive Control for Quadrotors with An Analytically Derived Koopman Model

Santosh M. Rajkumar¹, Sheng Cheng², Naira Hovakimyan², and Debdipta Goswami¹

Abstract—This letter presents a Koopman-theoretic lifted linear parameter-varying (LPV) system with countably infinite dimensions to model the nonlinear dynamics of a quadrotor on SE(3) for facilitating control design. The LPV system evolves in time in the space of the observables, called the lifted space. A primary challenge in utilizing the Koopman-based linearization is identifying a set of observables that can adequately span the lifted space, with the majority of the current methods using data to learn these observables. In this study, we analytically derive the observables for the quadrotor dynamics on SE(3) to formulate the lifted LPV system. The lifted LPV system has a countably infinite dimension which is then truncated for practical control design. The truncation is analytically justified by showing vanishing residual property in a bounded trajectory regime. The LPV system is then approximated as a linear time-invariant (LTI) system with a set of virtual control inputs. The controllability of the lifted LTI system is translatable to the true quadrotor system on SE(3). A linear model-predictive control (LMPC) scheme is formulated and implemented in numerical simulations employing this LTI framework for various tracking problems, with attention given to the potential for real-time implementation.

I. INTRODUCTION

Quadrotors are widely used in unmanned aerial systems (UAS) for their agility and versatility, particularly for missions that require tracking complex trajectories in real-time. Effective trajectory-tracking controllers are essential for performing high-speed maneuvers in complex environments. However, specific challenges such as nonlinear dynamics, aerodynamic influences, and actuation constraints are frequently encountered in the agile flight of quadrotors. Nonlinear Model Predictive Control (NMPC) has shown promise in addressing these challenges due to its predictive nature, but it is computationally intensive, especially for low-end micro unmanned aerial vehicles (micro-UAVs) [1]. An alternative approach involves using linearized quadrotor dynamics with Linear Model Predictive Control (LMPC) to reduce the computational load. But traditional linearization such as [2], [3] are valid only for a small domain around a reference trajectory and not suitable for agile flight as accuracy drops with farther deviation from the reference. Recent advances in Koopman operator theory provides a practical way to linearly embed a nonlinear system in an infinite-dimensional space of observable functions which

can then be truncated for a finite-dimensional representation [4]–[6]. The Koopman linear representation has improved the effectiveness of linear controllers in complex scenarios [7], [8]. However, state-of-the-art Koopman-based methods rely on a rich set of trajectory data with random control inputs to identify the linear dynamics in the latent space [9]–[11]. On the other hand, a model-based approach has proved beneficial in embedding the rigid body attitude dynamics on SO(3) linearly in a space of Koopman observables [12]. This is extended in [13] for quadrotor dynamics on SE(3) to incorporate linear position, velocity, and thrust. The embedding in [13] uses dynamic compensation for the body-frame linear velocity dynamics in order to get a simplified linear control, but in turn makes LMPC formulation with quadratic control cost difficult.

This letter provides an alternative Koopman linear embedding of quadrotor dynamics on SE(3) by analytically derived observable functions that span a Koopman-invariant subspace. This method does not require snapshot data to find the linear embedding and therefore can be used for LMPC without any training data collected *a priori*. Furthermore, this embedding uses linear velocity with respect to inertial frame and does not require dynamic compensation for total thrust [13]. The embedded linear parameter-varying (LPV) model is then approximated using a linear time-invariant (LTI) system without any loss of controllability with state-dependent control. The approximate LTI model, with a virtual control approximating the state-dependent control, is then used for trajectory tracking tasks through a properly curated LMPC scheme.

The contributions of this letter are as follows: (1) development of a countably infinite-dimensional Koopman linear embedding of quadrotor dynamics on SE(3) without relying on the dynamic compensation of the linear velocity; (2) analytical justification of the truncated embedding by establishing vanishing residual property; (3) proof of the controllability-retention in such linear embedding; (4) design and validation of a trajectory tracking controller via LMPC. To the best of our knowledge, this is the first attempt in implementing LMPC for trajectory tracking using an analytically derived Koopman-based lifted linear formulation of quadrotor dynamics.

Organization of This Letter: Section II gives an overview of quadrotor dynamics on SE(3) and Koopman operator. Section III derives the observables for lifted linear embedding, proves the vanishing residual property, presents retention of controllability, and formulates the LMPC problem. Section IV presents numerical simulation results illustrating the performance of the lifted linear model in approximating the quadrotor dynamics, and tracking control with the LMPC scheme. Finally, Section V presents concluding remarks.

This work is supported by the OSU departmental startup fund, NASA cooperative agreement (80NSSC22M0070), AFOSR (FA9550-21-1-0411), NSF-AoF Robust Intelligence (2133656), and NSF SLES (2331878)

¹ Authors are with the Department of Mechanical and Aerospace Engineering, The Ohio State University, Columbus, OH, 43210, USA. Email: {rajkumar.36, goswami.78}@osu.edu

² Authors are with the Department of Mechanical and Aerospace Engineering, University of Illinois, Urbana-Champaign, IL, USA. Email: {chengs, nhovakim}@illinois.edu

II. MATHEMATICAL PRELIMINARIES

A. Quadrotor Dynamics

Consider a quadrotor model with an inertial frame of reference $\mathcal{I}_{\text{ref}} \triangleq \{\vec{e}_1, \vec{e}_2, \vec{e}_3\}$ and a body-fixed frame $\mathcal{B}_{\text{ref}} \triangleq \{\vec{b}_1, \vec{b}_2, \vec{b}_3\}$ as depicted in Fig. 1. The quadrotor is modeled with four identical rotors positioned at the corners of a square that generate thrust perpendicular to the plane of the square in the \vec{b}_3 direction. The center of mass of the quadrotor lies at the origin of the body fixed frame. Define

$\mathbf{x} \in \mathbb{R}^3$: position of the center of mass in \mathcal{I}_{ref}

$\mathbf{v} \in \mathbb{R}^3$: the velocity of the center of mass in \mathcal{I}_{ref}

$\mathbf{R} \in SO(3)$: rotation matrix from \mathcal{B}_{ref} to \mathcal{I}_{ref}

$\boldsymbol{\omega} \in \mathbb{R}^3$: angular velocity in \mathcal{B}_{ref}

$\mathbf{M} \in \mathbb{R}^3$: total moment in \mathcal{B}_{ref}

$\mathbf{J} \in \mathbb{R}^{3 \times 3}$: inertia matrix with respect to \mathcal{B}_{ref}

$f \in \mathbb{R}$: the total thrust ($f = f_1 + f_2 + f_3 + f_4$)

$m \in \mathbb{R}$: total mass of the quadrotor

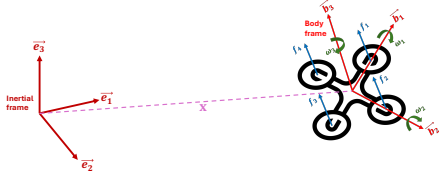


Fig. 1: Quadrotor Model

The quadrotor's configuration is defined by the location of its center of mass and its attitude with respect to the inertial frame. Therefore, the set of all possible configurations of the quadrotor is described by the special Euclidean group $SE(3)$ containing the special orthogonal group $SO(3) = \{\mathbf{R} \in \mathbb{R}^{3 \times 3} \mid \mathbf{R}^T \mathbf{R} = \mathbf{I} \ \& \ \det(\mathbf{R}) = 1\}$ and the position vector \mathbf{x} .

Considering f and $\mathbf{M} = [M_1 \ M_2 \ M_3]^T$ as the control inputs to the quadrotor, the governing equations of motion can be written as [14]

$$\dot{\mathbf{x}} = \mathbf{v}, \quad \dot{\mathbf{v}} = -g\vec{e}_3 + \frac{f}{m}\mathbf{R}\vec{e}_3, \quad \dot{\mathbf{R}} = \mathbf{R}\boldsymbol{\omega}^\times, \quad \dot{\boldsymbol{\omega}} = \mathfrak{J}\bar{\mathbf{M}}, \quad (1)$$

where $\mathfrak{J} = \mathbf{J}^{-1}$, $\bar{\mathbf{M}} = -\boldsymbol{\omega}^\times \mathbf{J} \boldsymbol{\omega} + \mathbf{M}$, and $(\cdot)^\times : \mathbb{R}^3 \rightarrow \mathfrak{so}(3)$ with the condition that $\mathbf{p}^\times \mathbf{q} = \mathbf{p} \times \mathbf{q}$. More details on the dynamics of the quadrotor model can be found in [14].

B. Koopman Operator Theory

The Koopman operator describes how a dynamical system evolves over time by using functions defined in a Banach space [15]. Consider a controlled dynamical system,

$$\dot{\mathbf{x}}(t) = \mathbf{f}(\mathbf{x}(t), \mathbf{u}(t)), \quad (2)$$

on a manifold $\mathcal{M} \in \mathbb{R}^n$ driven by a control from an admissible set \mathcal{U} , i.e., $\mathbf{x} \in \mathcal{M}$ and $\mathbf{f} : \mathcal{M} \times \mathcal{U} \rightarrow \mathcal{M}$. Let $\Phi_{\mathbf{u}}(t, \mathbf{x})$ be the flow map of the system (2) at time $t > 0$ starting from an initial state \mathbf{x} under a control $\mathbf{u}(\cdot)$. A measurable function $\varphi : \mathbb{X} \rightarrow \mathbb{C}$ is called an observable of the dynamical system (2). Let \mathcal{F} be a Banach space of real-valued observables $\varphi : \mathbb{X} \rightarrow \mathbb{R}$. The

continuous time Koopman operator associated with the control $\mathbf{u}(\cdot)$ is defined as $\mathcal{K}_{\mathbf{u}}^t : \mathcal{F} \rightarrow \mathcal{F}$ such that

$$(\mathcal{K}_{\mathbf{u}}^t \varphi)(\cdot) = \varphi \circ \Phi_{\mathbf{u}}(t, \cdot), \quad (3)$$

where \circ denotes the function composition. Notably, the Koopman operator is linear over its arguments, i.e., the observable functions, albeit being an infinite-dimensional one. The infinitesimal generator of $\mathcal{K}_{\mathbf{u}}^t$, i.e., $\lim_{t \rightarrow 0} \frac{\mathcal{K}_{\mathbf{u}}^t - I}{t}$, is $\mathbf{f}(\cdot, \mathbf{u}) \cdot \nabla = L_{\mathbf{f}(\cdot, \mathbf{u})}$ [5], where I is the identity operator and $L_{\mathbf{f}(\cdot, \mathbf{u})}$ is the Lie derivative with respect to $\mathbf{f}(\cdot, \mathbf{u})$. Using the operator limit on (3) yields

$$\dot{\varphi} = L_{\mathbf{f}(\cdot, \mathbf{u})} \varphi = \mathbf{f}(\cdot, \mathbf{u}) \cdot \nabla \varphi. \quad (4)$$

If the system (2) has the special control-affine form

$$\dot{\mathbf{x}} = \mathbf{f}(\mathbf{x}) + \sum_{i=1}^m \mathbf{g}_i(\mathbf{x}) u_i, \quad (5)$$

then (4) becomes

$$\dot{\varphi} = L_{\mathbf{f}} \varphi + \sum_{i=1}^m u_i L_{\mathbf{g}_i} \varphi. \quad (6)$$

Now, let \mathcal{F} be the span of a countable collection of real-valued observables $\alpha(\cdot) = \{\alpha_i(\cdot), \ i = 1, \dots\}$ where $\alpha_i : \mathcal{M} \rightarrow \mathbb{R}^m$. If \mathcal{F} is invariant under $L_{\mathbf{f}}$, i.e., in turn invariant under $\mathcal{K}_{\mathbf{u}}^t$, then the derivative of $\alpha = [\alpha_1, \alpha_2, \dots]$, with a slight abuse of notation, becomes

$$\dot{\alpha} = \mathbf{A}\alpha + \mathcal{B}(\alpha)\mathbf{u} \Rightarrow \dot{\mathbf{z}} = \mathbf{A}\mathbf{z} + \mathcal{B}(\mathbf{z})\mathbf{u}, \quad (7)$$

by expanding (6) in the vector form and using the property of invariance [16]. The lifted state $\mathbf{z} \triangleq \alpha(\mathbf{x})$ now contains countably infinite dimension which needs to be truncated to a finite-dimensional lifted state $\mathbf{X} = [z_1, z_2, \dots, z_d]^T$ for any practical application preferably with a guarantee of vanishing residuals. However, identifying an appropriate set of observables to span the lifted space \mathcal{F} can be challenging, as there is no systematic method to construct these functions universally.

III. LIFTED KOOPMAN LINEAR EMBEDDING FOR QUADROTOR DYNAMICS ON $SE(3)$

It is evident from (1) that the quadrotor dynamics is control affine with 4-dimensional control $\bar{\mathbf{u}} = [f, \bar{\mathbf{M}}]^T$. The objective is to find a set of observables $\alpha(\cdot)$ that spans an invariant subset of the corresponding $L_{\mathbf{f}}$ and provides a quasilinear form (7).

A. Observable Formulation

Consider the following set of observables for the quadrotor system,

$$\alpha = \left(\{\mathbf{h}_k\}_{k=1}^\infty, \{\mathbf{y}_k\}_{k=1}^\infty, \{\mathbf{p}_k\}_{k=1}^\infty, \{\mathbf{z}_j\}_{j=1}^\infty \right), \quad (8)$$

where, $\mathbf{h}_k, \mathbf{y}_k, \mathbf{p}_k \in \mathbb{R}^3$ and $\mathbf{z}_j \in \mathbb{R}^9$. Here, the observables $\mathbf{h}_k, \mathbf{y}_k, \mathbf{p}_k$, and \mathbf{z}_j are associated with the gravitational acceleration, linear velocity, position, and rotational dynamics respectively. Define the observables as follows,

$$\mathbf{h}_k = ((\boldsymbol{\omega}^\times)^T)^{k-1} \mathbf{R}^T \begin{bmatrix} 0 & 0 & g \end{bmatrix}^T, \quad \mathbf{y}_k = ((\boldsymbol{\omega}^\times)^T)^{k-1} \mathbf{R}^T \mathbf{v}, \quad (9)$$

$$\mathbf{p}_k = ((\boldsymbol{\omega}^\times)^T)^{k-1} \mathbf{R}^T \mathbf{x}, \quad \mathbf{z}_j = \text{vec}(\mathbf{R}(\boldsymbol{\omega}^\times)^{j-1}).$$

The rationale behind using two different indexing k and j here is that the rotational dynamics of the quadrotor is spanned by

the observables with the latter indices. Using $\Omega \triangleq \omega^\times$, for any k and j , the recurrent relations are

$$\begin{aligned} \mathbf{h}_{k+1} &= (\Omega^T)^k \mathbf{h}_k, & \mathbf{y}_{k+1} &= (\Omega^T)^k \mathbf{y}_k, \\ \mathbf{p}_{k+1} &= (\Omega^T)^k \mathbf{p}_k, & \mathbf{z}_{j+1} &= \text{vec}(\mathbf{R}\Omega^j). \end{aligned} \quad (10)$$

The span of α , as shown in the next theorem, is an invariant subspace of $L_{\mathcal{F}}$.

Theorem 1: The following countably infinite collection of observables

$$\alpha = \left(\{\mathbf{h}_k\}_{k=1}^\infty, \{\mathbf{y}_k\}_{k=1}^\infty, \{\mathbf{p}_k\}_{k=1}^\infty, \{\mathbf{z}_j\}_{j=1}^\infty \right)$$

span an invariant subspace of $L_{\mathcal{F}}$ for quadrotor dynamics with control $\bar{\mathbf{u}} = [f, \bar{\mathbf{M}}]^T$ and yields a quasilinear form (7).

Proof: Using (9) and (10) the evolution of the observables in the lifted space are given as (with $\hat{\mathbf{f}} = [0, 0, f]^T$, $\mathcal{S}_i^k = (\Omega^T)^{i-1} \dot{\Omega}^T (\Omega^T)^{k-1-i}$, and $\sigma_k = (\Omega^T)^{k-1}$),

$$\dot{\mathbf{h}}_1 = \mathbf{h}_2, \quad \dot{\mathbf{h}}_k = \mathbf{h}_{k+1} + \sum_{i=1}^{k-1} \mathcal{S}_i^k \mathbf{h}_1 \quad (k > 1), \quad (11)$$

$$\dot{\mathbf{y}}_1 = \mathbf{y}_2 + \mathbf{h}_1 + \frac{\hat{\mathbf{f}}}{m}, \quad \dot{\mathbf{y}}_k = \mathbf{y}_{k+1} + \mathbf{h}_k + \frac{\sigma_k \hat{\mathbf{f}}}{m} + \sum_{i=1}^{k-1} \mathcal{S}_i^k \mathbf{y}_1 \quad (k > 1),$$

$$\dot{\mathbf{p}}_1 = \mathbf{p}_2 + \mathbf{y}_1, \quad \dot{\mathbf{p}}_k = \mathbf{p}_{k+1} + \mathbf{y}_k + \sum_{i=1}^{k-1} \mathcal{S}_i^k \mathbf{p}_1 \quad (k > 1),$$

$$\dot{\mathbf{z}}_1 = \mathbf{z}_2, \quad \text{and } \dot{\mathbf{z}}_j = \mathbf{z}_{j+1} + \text{vec}(\mathbf{R} \sum_{i=1}^{j-1} (\Omega^T)^{i-1} \dot{\Omega} (\Omega^T)^{j-1-i}), \quad (j > 1).$$

For $k = M$ and $j = N$, by taking $M \rightarrow \infty$ and $N \rightarrow \infty$, we obtain countably infinite number of observables as defined in (9) that span the lifted space. Further, to prove the quasilinear form of (7), we truncate the number of observable beforehand to circumvent the inconvenience of infinite matrices. Let $\mathbf{X} = [\mathbf{p}_1 \dots \mathbf{p}_M \mathbf{y}_1 \dots \mathbf{y}_M \mathbf{h}_1 \dots \mathbf{h}_M \mathbf{z}_1 \dots \mathbf{z}_N]^T \in \mathbb{R}^{9M+9N}$ be the state vector in the lifted space of the observables. Since $\bar{\mathbf{u}} = [f \quad \bar{\mathbf{M}}]^T \in \mathbb{R}^4$, with $\mathbf{u} = [f \quad \mathbf{M}]^T = \bar{\mathbf{u}} + [0 \quad \omega^\times \mathbf{J}\omega]^T$, we obtain the dynamics of the quadrotor in the lifted space from (11) as,

$$\dot{\mathbf{X}} = \mathbf{A}\mathbf{X} + \mathcal{B}(\mathbf{X})\bar{\mathbf{u}}, \quad (12)$$

where

$$\begin{aligned} \mathbf{A} &= \begin{bmatrix} \mathbf{A}_p & \mathbf{0} \\ \mathbf{0} & \mathbf{A}_a \end{bmatrix}, \quad \mathbf{A}_p \in \mathbb{R}^{9M \times 9M}, \quad \mathbf{A}_a \in \mathbb{R}^{9N \times 9N}, \\ \mathcal{B} &= \begin{bmatrix} \mathcal{B}_p^T & \mathcal{B}_a^T \end{bmatrix}^T, \quad \mathcal{B}_p \in \mathbb{R}^{9M \times 4}, \quad \mathcal{B}_a \in \mathbb{R}^{9N \times 4}, \\ \mathbf{A}_p &= \begin{bmatrix} \mathbf{0} & \mathbf{I}_3 & \mathbf{0} & \mathbf{I}_3 & \mathbf{0} & \dots & \dots & \dots & \dots & \mathbf{0} \\ \mathbf{0} & \mathbf{0} & \ddots & \mathbf{0} & \ddots & \mathbf{0} & \dots & \dots & \dots & \mathbf{0} \\ \mathbf{0} & \mathbf{0} & \mathbf{0} & \mathbf{0} & \mathbf{0} & \mathbf{0} & \mathbf{0} & \mathbf{0} & \mathbf{0} & \mathbf{0} \\ \mathbf{0} & \mathbf{0} & \mathbf{0} & \mathbf{0} & \mathbf{I}_3 & \mathbf{0} & \mathbf{I}_3 & \mathbf{0} & \dots & \mathbf{0} \\ \mathbf{0} & \mathbf{0} & \mathbf{0} & \mathbf{0} & \mathbf{0} & \ddots & \mathbf{0} & \ddots & \mathbf{0} & \mathbf{0} \\ \mathbf{0} & \mathbf{0} & \mathbf{0} & \mathbf{0} & \mathbf{0} & \mathbf{0} & \mathbf{0} & \mathbf{0} & \mathbf{0} & \mathbf{0} \\ \mathbf{0} & \mathbf{0} & \mathbf{0} & \mathbf{0} & \mathbf{0} & \mathbf{0} & \mathbf{0} & \mathbf{0} & \mathbf{I}_3 & \mathbf{0} \\ \mathbf{0} & \mathbf{0} & \mathbf{0} & \mathbf{0} & \mathbf{0} & \mathbf{0} & \mathbf{0} & \mathbf{0} & \mathbf{0} & \mathbf{0} \end{bmatrix}, \\ \mathbf{A}_a &= \begin{bmatrix} \mathbf{0} & \mathbf{I}_9 & \mathbf{0} & \dots & \mathbf{0} \\ \mathbf{0} & \mathbf{0} & \mathbf{I}_9 & \dots & \mathbf{0} \\ \vdots & \vdots & \vdots & \ddots & \vdots \\ \mathbf{0} & \mathbf{0} & \mathbf{0} & \mathbf{0} & \mathbf{I}_9 \\ \mathbf{0} & \mathbf{0} & \mathbf{0} & \dots & \mathbf{0} \end{bmatrix}, \end{aligned}$$

$$\mathcal{B}_p = \begin{bmatrix} \mathbf{p}_0^T & \dots & \mathbf{p}_{M-1}^T & \mathbf{y}_0^T & \dots & \mathbf{y}_{M-1}^T & \mathbf{b}_0^T & \dots & \mathbf{b}_{M-1}^T \end{bmatrix}^T,$$

$$\mathcal{B}_a = \begin{bmatrix} \mathcal{G}_0^T & \mathcal{G}_1^T & \dots & \mathcal{G}_{N-1}^T \end{bmatrix}^T, \quad \text{with}$$

$$\mathbf{b}_k = \begin{bmatrix} \mathbf{0}_{3 \times 1} & \mathbf{H}_k \end{bmatrix}, \quad \mathbf{y}_k = \begin{bmatrix} \mathcal{Y}_{k+1} & \mathbf{Y}_k \end{bmatrix}, \quad \mathcal{Y}_k = \frac{\sigma_k \bar{\mathbf{e}}_3}{m},$$

$$\mathbf{p}_k = \begin{bmatrix} \mathbf{0}_{3 \times 1} & \mathbf{P}_k \end{bmatrix}, \quad \mathbf{H}_0 = \mathbf{P}_0 = \mathbf{0}_{3 \times 4}, \quad \mathbf{Y}_0 = \mathbf{0}_{3 \times 3},$$

$$\mathbf{H}_k = \sum_{i=1}^k \bar{\mathcal{S}}_i^k(\mathbf{h}_1) \mathfrak{Z}, \quad (k > 0), \quad \mathbf{Y}_k = \sum_{i=1}^k \bar{\mathcal{S}}_i^k(\mathbf{y}_1) \mathfrak{Z}, \quad (k > 0),$$

$$\mathbf{P}_k = \sum_{i=1}^k \bar{\mathcal{S}}_i^k(\mathbf{p}_1) \mathfrak{Z}, \quad (k > 0), \quad \bar{\mathcal{S}}_i^k(\mathbf{a}) = (\Omega^T)^{i-1} ((\Omega^T)^{k-i} \mathbf{a})^\times,$$

$$\mathcal{G}_k = \begin{bmatrix} \mathbf{0}_{9 \times 1} & \mathbf{G}_k \end{bmatrix}, \quad \mathbf{G}_0 = \mathbf{0}_{9 \times 3},$$

$$\mathbf{G}_k = \begin{bmatrix} \mathbf{g}_{k1} & \mathbf{g}_{k2} & \mathbf{g}_{k3} \end{bmatrix}, \quad (k > 0), \quad \mathfrak{Z} = \begin{bmatrix} \mathbf{j}_1 & \mathbf{j}_2 & \mathbf{j}_3 \end{bmatrix},$$

$$\mathbf{g}_{k_m} = \text{vec}(\mathbf{R} \sum_{j=1}^k \Omega^{j-1} \mathbf{j}_m^\times \Omega^{i-j}), \quad (m = 1, 2, 3).$$

This completes the proof. \blacksquare

B. Vanishing Residual Property

To apply the truncated model (12) for MPC, we must ensure that the omitted residual terms and their derivatives vanishes as $j, k \rightarrow \infty$. Let us define a truncated state-space $\bar{\mathcal{M}} = \{[\mathbf{x}, \mathbf{v}, \mathbf{R}, \omega] \in \mathcal{M} : \|\mathbf{x}\| \leq \bar{x}, \|\mathbf{v}\| \leq \bar{v}, \|\omega\| \leq \bar{\omega}\}$.

Theorem 2: If $\bar{\omega} = 1/\sqrt{2}$ and $\|\bar{\mathbf{u}}\| \leq \bar{u}$, then

$$\lim_{k \rightarrow \infty} \mathbf{h}_k = 0, \quad \lim_{k \rightarrow \infty} \mathbf{y}_k = 0, \quad \lim_{k \rightarrow \infty} \mathbf{p}_k = 0, \quad \lim_{j \rightarrow \infty} \mathbf{z}_j = 0, \quad \text{and} \quad (13)$$

$$\lim_{k \rightarrow \infty} \dot{\mathbf{h}}_k = 0, \quad \lim_{k \rightarrow \infty} \dot{\mathbf{y}}_k = 0, \quad \lim_{k \rightarrow \infty} \dot{\mathbf{p}}_k = 0, \quad \lim_{j \rightarrow \infty} \dot{\mathbf{z}}_j = 0, \quad (14)$$

for $[\mathbf{x}, \mathbf{v}, \mathbf{R}, \omega] \in \bar{\mathcal{M}}$.

Proof: From (9), $\|\mathbf{y}_k\| = \|((\omega^\times)^T)^{k-1} \mathbf{R}^T \mathbf{v}\| \leq \|\omega\|^{k-1} \|\mathbf{v}\|$, where the last inequality is due to Cauchy-Schwartz and the fact that $\|\mathbf{R}\| = 1$. Since $\|\omega\| \leq \bar{\omega} = 1/\sqrt{2}$, then $\|\omega\|^k \|\mathbf{v}\|$ goes to 0 as $k \rightarrow \infty$. Hence, we have $\lim_{k \rightarrow \infty} \mathbf{y}_k = 0$. In similar fashion, we can show,

$$\lim_{k \rightarrow \infty} \mathbf{h}_k = 0, \quad \lim_{k \rightarrow \infty} \mathbf{p}_k = 0, \quad \lim_{j \rightarrow \infty} \mathbf{z}_j = 0, \quad (15)$$

From (11),

$$\dot{\mathbf{y}}_k = \mathbf{y}_{k+1} + \mathbf{h}_k + \frac{\sigma_k \hat{\mathbf{f}}}{m} + \sum_{i=1}^{k-1} \mathcal{S}_i^k \mathbf{y}_1 \quad (k > 1), \quad (16)$$

where $\Omega = \omega^\times$. The first three terms of the RHS goes to zero by virtue of (13) as $k \rightarrow \infty$. The summation in the last term contains $\mathcal{S}_i^k \mathbf{y}_1$ where, for each term,

$$\|\mathcal{S}_i^k \mathbf{y}_1\| \leq \|\omega\|^{k-2} \|\dot{\omega}^\times\| \|\mathbf{y}_1\|. \quad \text{This, in turn, yields}$$

$$\left\| \sum_{i=1}^{k-1} \mathcal{S}_i^k \mathbf{y}_1 \right\| \leq (k-1) \|\omega\|^{k-2} \|\dot{\omega}^\times\| \|\mathbf{y}_1\|.$$

$$\text{Now, } \|\dot{\omega}^\times\| = \|\mathfrak{Z} \bar{\mathbf{M}}^\times\| \leq \|\mathfrak{Z}\| \|\bar{\mathbf{M}}\| \leq \|\mathfrak{Z}\| \bar{u},$$

where the first equality follows from (1) and the last two inequalities are due to Cauchy-Schwartz. This inequality, along with $\|\omega\| \leq \bar{\omega} = 1/\sqrt{2}$, helps us to conclude that

$\lim_{k \rightarrow \infty} \sum_{i=1}^{k-1} \mathbf{S}_i^k \mathbf{y}_1 = 0$. Hence, $\lim_{k \rightarrow \infty} \dot{\mathbf{y}}_k = 0$, $\lim_{k \rightarrow \infty} \dot{\mathbf{h}}_k = 0$, and $\lim_{k \rightarrow \infty} \dot{\mathbf{p}}_k = 0$

For $\dot{\mathbf{z}}_j$, the summation term is vectorized. Using the orthogonal property of \mathbf{R} and the definition of matrix Frobenius norm, it can be shown that $\|\mathbf{R}\omega^{\times j}\|_F = \|\text{vec}(\omega^{\times j})\|$. Now from the Cauchy-Schwartz inequality

$$\|\omega^{\times j}\|_F \leq \|\omega^{\times}\|_F^j = \|\text{vec}(\omega^{\times})\|^j \leq \sqrt{2}^j \|\omega\|^j.$$

Hence, $\|\text{vec}(\mathbf{R}\omega^{\times j})\| \leq \|\text{vec}(\omega^{\times})\|^j \leq \sqrt{2}^j \|\omega\|^j$. These two inequalities, along with $\|\omega\| \leq \bar{\omega} = 1/\sqrt{2}$, imply that $(j-1)\|\text{vec}(\omega^{\times})^{j-2}\|$ will also go to zero as $j \rightarrow \infty$, thereby proving $\lim_{j \rightarrow \infty} \dot{\mathbf{z}}_j = 0$. This completes the proof. \blacksquare

Remark 1: For most practical purposes, the angular rate ω , velocity \mathbf{v} , and actuation $\bar{\mathbf{u}}$ will be constrained. Also, we can normalize ω by a factor of $\sqrt{2} \max(\|\omega\|)$ to keep the normalized ω below $1/\sqrt{2}$.

C. Lifted LTI System

We introduce a state-dependent control of the form,

$$\mathbf{U} = \begin{bmatrix} \mathbf{U}_p^T & \mathbf{U}_a^T \end{bmatrix}^T \in \mathbb{R}^{9(M+N)-15}, \quad (17)$$

where $\mathbf{U}_p = [\mathbf{u}_{h_1}, \dots, \mathbf{u}_{h_{M-1}}, \mathbf{u}_{y_0}, \dots, \mathbf{u}_{y_{M-1}}, \mathbf{u}_{p_1}, \dots, \mathbf{u}_{p_{M-1}}]^T$ and $\mathbf{U}_a = [\mathbf{u}_{a_1}, \dots, \mathbf{u}_{a_{N-1}}]^T$, with $\mathbf{u}_{h_k} = \mathfrak{h}_k \bar{\mathbf{u}}$, $\mathbf{u}_{y_k} = \mathfrak{y}_k \bar{\mathbf{u}}$, $\mathbf{u}_{p_k} = \mathfrak{p}_k \bar{\mathbf{u}}$, and $\mathbf{u}_{a_k} = \mathfrak{a}_k \bar{\mathbf{u}}$. With the control in (17), we can represent (12) as an LTI system with state-dependent control as,

$$\dot{\mathbf{X}} = \mathbf{A}\mathbf{X} + \bar{\mathbf{B}}\mathbf{U}(\mathbf{X}), \quad \text{where} \quad (18)$$

$$\bar{\mathbf{B}} = \begin{bmatrix} \begin{bmatrix} \mathbf{0}_{3 \times 3(M-1)} & \mathbf{0}_{3 \times 3} & \mathbf{0}_{3M \times 9(N-1)} \\ \mathbf{I}_{3(M-1)} & \mathbf{0}_{3 \times 3} & \mathbf{0} \end{bmatrix} \\ \begin{bmatrix} \mathbf{0}_{3M \times 3(M-1)} & \mathbf{I}_{3M} & \mathbf{0}_{3M \times 9(N-1)} \\ \mathbf{0}_{3M \times 9(N-1)} & \mathbf{0}_{3M \times 9(N-1)} & \mathbf{0}_{3M \times 9(N-1)} \end{bmatrix} \\ \begin{bmatrix} \mathbf{0}_{9(N-1) \times 9M-6} & \mathbf{I}_{9(N-1)} & \mathbf{0} \end{bmatrix} \end{bmatrix} \in \mathbb{R}^{9(M+N) \times 9(M+N)-15} \quad (19)$$

$$\text{with } \bar{\mathbf{B}}_* = \begin{bmatrix} \mathbf{0}_{3 \times 3(M-1)} & \mathbf{0}_{3 \times 3M} & \mathbf{0}_{3 \times 3(M-1)} \\ \mathbf{0}_{3(M-1) \times 3(M-1)} & \mathbf{0}_{3(M-1) \times 3M} & \mathbf{I}_{3(M-1)} \\ \mathbf{0}_{9 \times 3(M-1)} & \mathbf{0}_{9 \times 3M} & \mathbf{0}_{9 \times 3(M-1)} \end{bmatrix}.$$

Clearly, $\bar{\mathbf{B}}$ is a matrix with constant entries resulting in an LTI representation of (12) with high-dimensional state-dependent control \mathbf{U} .

D. Virtual Control for the Lifted LTI System

Suppose that we have a high-dimensional virtual control $\mathbf{U} \in \mathbb{R}^{9(M+N)-15}$ for the lifted LTI system (18) representing \mathbf{U} , we would like to recover the control $\bar{\mathbf{u}}$. Recovering $\bar{\mathbf{u}}$ is an optimization problem,

$$\min_{\bar{\mathbf{u}}} \mathcal{J} = (\mathbf{B}\bar{\mathbf{u}} - \bar{\mathbf{B}}\mathbf{U})^T (\mathbf{B}\bar{\mathbf{u}} - \bar{\mathbf{B}}\mathbf{U}). \quad (20)$$

Essentially, (20) is a least-square problem with a solution for $\bar{\mathbf{u}}$ is given as,

$$\bar{\mathbf{u}} = \mathbf{B}^\dagger \bar{\mathbf{B}}\mathbf{U}, \quad (21)$$

where \mathbf{B}^\dagger is the Moore-Penrose pseudo-inverse of \mathbf{B} . This solution is unique if and only if

$$\mathbf{B}^\dagger = (\mathbf{B}^T \mathbf{B})^{-1} \mathbf{B}^T. \quad (22)$$

Lemma 1: The solution to the least squared problem in (20) is unique if the moment of inertia matrix \mathbf{J} is invertible.

Proof: This can be proved by checking the linear independence of the columns of \mathbf{B} so that $(\mathbf{B}^T \mathbf{B})^{-1}$ exists. The first column of \mathbf{B} is simply $[\mathbf{0}_{3M \times 1}, \{\mathcal{Y}_j\}_{j=1}^M, \mathbf{0}_{(3M+9N) \times 1}]^T$. Further, the columns two to four of \mathbf{B} is simply a matrix $[\{\mathbf{H}_i^T\}_{i=0}^{M-1}, \{\mathbf{Y}_i^T\}_{i=0}^{M-1}, \{\mathbf{P}_i^T\}_{i=0}^{M-1}, \{\mathbf{G}_i^T\}_{i=0}^{N-1}]^T$. The entity \mathbf{G}_1 depends only on \mathbf{R} and \mathfrak{Z} , and \mathcal{Y}_1 doesn't depend on any state of the nonlinear dynamics. Hence, \mathbf{B} has linearly independent columns as long as \mathbf{J} is invertible, completing the proof. \blacksquare Therefore, by designing a virtual control action \mathbf{U} for the lifted LTI system, we can obtain the control \mathbf{u} (from $\bar{\mathbf{u}}$) for the quadrotor dynamics in the least-squared sense.

E. Controllability in the Lifted Space

Lemma 2: The lifted LTI (18) is controllable.

Proof: The $(9M+9N)$ -dimensional lifted LTI system in (18) is controllable if the following controllability matrix C with $\mathbf{A}\bar{\mathbf{B}} = \hat{\mathbf{B}}$ is of full row rank:

$$C = [\bar{\mathbf{B}} \quad \hat{\mathbf{B}} \quad \mathbf{A}\hat{\mathbf{B}} \quad \dots \quad \mathbf{A}^{9(M+N)-2}\hat{\mathbf{B}}]. \quad (23)$$

It should be noted that $\bar{\mathbf{B}}$ by construction has $\gamma = 9(M+N) - 15$ linearly independent columns. Further, $\mathbf{A}^j \bar{\mathbf{B}}$ has $\alpha + \beta$ linearly independent columns, where,

$$\alpha = 9(N-1-j), \quad \text{for } j = 0, 1, \dots, N-2$$

$$\beta = \begin{cases} 9(M-1-j) & , \text{ for } j = 0, 1, \dots, M-3 \\ 12 & , \text{ for } j = M-2 \\ 6 & , \text{ for } j = M-1 \\ 3 & , \text{ for } j = M. \end{cases}$$

Therefore, C has in total $\mathcal{L}_c = \gamma + \sum_{j=0}^{N-2} 9(N-1-j) + \sum_{j=0}^{M-3} 9(M-1-j) + 21$ non-zero columns, with $\mathcal{L}_c \geq 9(M+N)$ for $N \geq 2$ and $M \geq 3$. Given that each row of C contains at least one non-zero element, it is possible to identify $9(M+N)$ linearly independent non-zero columns, thereby ensuring the full row rank of C . \blacksquare

Now that (18) is controllable, we can design the virtual control \mathbf{U} and uniquely find out $\bar{\mathbf{u}}$ for the LPV system (12) using (21) with the hope that (12) is controllable as well.

Lemma 3: The LPV system (12) is controllable in $[t_0, t_f]$ if the moment of inertia matrix \mathbf{J} is invertible and quadrotor state is away from $\mathbf{x} = 0$, $\mathbf{v} = 0$, and $\omega = 0$.

Proof: The LPV system (12) is controllable at time t_0 subject to the existence of a finite time $t_f > t_0$ if the controllability gramian

$$\mathcal{W} = \int_{t_0}^{t_f} e^{\mathbf{A}\tau} \mathbf{B}(\mathbf{X}) \mathbf{B}(\mathbf{X})^T e^{\mathbf{A}^T \tau} d\tau \quad (24)$$

is non-singular. Next, \mathcal{W} is non-singular if and only if there exists no non-zero vector $\mathbf{w} \in \mathbb{R}^{9(M+N)}$ such that,

$$\mathbf{w}^T e^{\mathbf{A}t} \mathbf{B} = \mathbf{0} \implies \mathbf{w}^T \hat{C} = \mathbf{0}, \quad \forall t \in [t_0, t_f], \quad (25)$$

where, $\hat{C} = [\bar{\mathbf{B}} \quad \mathbf{A}\bar{\mathbf{B}} \quad \dots \quad \mathbf{A}^{9(M+N)-1}\bar{\mathbf{B}}]$ is the state-dependent controllability matrix. The full row-rank of \hat{C} for all for all $t \in [t_0, t_f]$ ensures it. Equivalently, if the matrix $[\mathbf{A} - \lambda \mathbf{I}] \mathbf{B}$ has full row-rank at each eigenvalue λ , \mathcal{W} is non-singular, and (12) is controllable for all $t \in [t_0, t_f]$ [17]. The system matrix \mathbf{A} is a nilpotent upper triangular matrix and by construction has $9(M+N-2)$ linearly independent rows. The linearly dependent

rows of \mathbf{A} have zero entries only. Therefore, $[\mathbf{A} - \lambda\mathbf{B}]$ has full row-rank if the rows of \mathbf{B} , corresponding to the rows of \mathbf{A} with all the zero entries, are linearly independent. In other words, the full row rank for all $t \in [t_0, t_f]$ of

$$\mathbf{C}_* = \begin{bmatrix} \mathbf{p}_{M-1}^T & \mathbf{v}_{M-1}^T & \mathbf{b}_{M-1}^T & \mathbf{G}_{N-1}^T \end{bmatrix}^T, \quad (\in \mathbb{R}^{18 \times 4}), \quad (26)$$

ensures controllability of (12). By composition, \mathbf{C}_* should possess full row rank for all $t \in [t_0, t_f]$ as long as \mathbf{J} is invertible and the states satisfy $\mathbf{x}, \mathbf{v}, \omega \neq \mathbf{0}$, completing the proof. ■

F. Linear Model Predictive Control (MPC)

Given the current state for the nonlinear quadrotor dynamics at time t , we use our observables to obtain the equivalent state $\mathbf{X}(t)$ in the lifted space. For a finite time horizon t_h , the LMPC scheme involves solving the optimal control problem (OCP) (27) to obtain the virtual control \mathbf{U} at t .

$$\begin{aligned} \min_{\mathbf{X}, \mathbf{U}} \mathcal{J}_* &= \int_0^{t_h} \|\mathbf{X} - \mathbf{X}_{ref}\|_{\mathbf{Q}}^2 + \|\mathbf{U} - \mathbf{U}_{ref}\|_{\mathbf{R}}^2 \\ \text{subject to: } \mathbf{X} &\in \mathcal{X}, \mathbf{U} \in \hat{\mathcal{U}} \\ \dot{\mathbf{X}} &= \mathbf{A}\mathbf{X} + \mathbf{B}\mathbf{U} \\ \mathbf{X}(0) &= \mathbf{X}(t), \end{aligned} \quad (27)$$

where \mathcal{X} is the set of admissible states, $\hat{\mathcal{U}}$ is the set of admissible control, \mathbf{X}_{ref} is the reference state translated from reference states for (1), \mathbf{U}_{ref} is the desired control, \mathbf{Q} is the weighting matrix for state cost, and \mathbf{R} is the weighting matrix for the control cost.

We can obtain \mathcal{X} from the bounds on the state of (1). For $\hat{\mathcal{U}}$, we need the bounds on the control in the lifted space. A bound on the control \mathbf{u}_b gives us corresponding bound $\bar{\mathbf{u}}_b$ at any time t . For any $\bar{\mathbf{u}}_b$, recovering the bound on the lifted space control \mathbf{U}_b is an optimization problem,

$$\min_{\mathbf{U}_b} \bar{\mathcal{J}} = (\mathbf{B}\bar{\mathbf{u}}_b - \bar{\mathbf{B}}\mathbf{U}_b)^T (\mathbf{B}\bar{\mathbf{u}}_b - \bar{\mathbf{B}}\mathbf{U}_b), \quad (28)$$

the solution to which in the least-squared sense is

$$\mathbf{U}_b = \bar{\mathbf{B}}^\dagger \mathbf{B}\bar{\mathbf{u}}_b, \quad (29)$$

where $\bar{\mathbf{B}}^\dagger$ is the Moore-Penrose pseudo-inverse of $\bar{\mathbf{B}}$. The solution (29) is unique as $\bar{\mathbf{B}}$ has linearly independent columns.

IV. NUMERICAL EXAMPLES

This section presents numerical simulations to validate the proposed Koopman-theoretic approximation of (1) as the lifted LPV model (12). We also demonstrate virtual control (\mathbf{U}) based on the lifted LTI model (18) using LMPC for trajectory tracking. Simulations are performed in MATLAB® 2023a on an Intel i-7 2.6 GHz MacBook. The parameters for the quadrotor model, chosen as per an in-house developed quadrotor are: $\mathbf{J} = \text{diag}([0.0023, 0.0026, 0.0032])$ kgm², and $m = 0.904$ kg.

The accuracy of the lifted-space dynamics model in comparison to the exact nonlinear model for the quadrotor was evaluated by measuring the approximation error. The approximation error (normalized) for position and velocity is given as $\|\mathbf{p} - \mathbf{q}\| / \|\mathbf{q}\|$ where \mathbf{p} obtained using (12) and \mathbf{q} computed using (1). The attitude approximation error is defined as $\Psi = \text{trace}(\mathbf{I}_3 - \mathbf{R}_q^T \mathbf{R}_p) / 2$ where \mathbf{R}_q obtained using

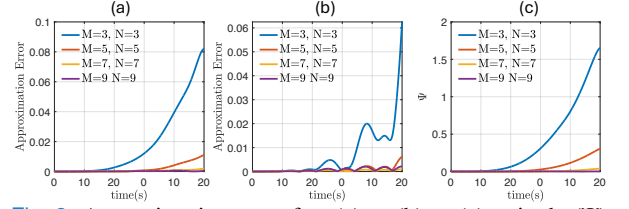


Fig. 2: Approximation error for: (a) \mathbf{x} , (b) \mathbf{v} , (c) attitude (Ψ)

(1) and \mathbf{R}_p computed using (12). A control signal with $f = 20mg \sin(t)$ and individual values of $\bar{\mathbf{M}}$ taking random values in $[-0.006, 0.006]$ as $0.001\xi(t) \sin(0.01t)$ used with initial conditions $\mathbf{R}(0) = \mathbf{I}_3$, $\omega(0) = [0.05, 0.05, 0.05]^T$, $\mathbf{x}(0) = [0.1, 0.1, 0.1]^T$, and $\mathbf{v}(0) = [0.1, 0.1, 0.1]^T$. Here, $\xi(t)$ is a random number picked from the uniform distribution $[-6, 6]$. Fig. 2 depicts variation of approximation error for \mathbf{x} , \mathbf{v} , and attitude for different values of M and N with time. As anticipated, increasing the dimension of the lifted space reduces the approximation error. However, regardless of the dimensions of M and N , the approximation error tends to grow over time due to the accumulation of the integral of the truncated terms. This finding necessitates implementation of finite horizon LMPC for more reliable control compared to conventional approaches like LQR control.

The LMPC scheme for quadrotor tracking control involves solving the OCP (27) at any time t to obtain $\mathbf{U}(t)$, and using (21) and current states to compute $\mathbf{u}(t)$. The OCP (27) is set up and solved using *acados* [18] with a time horizon $t_h = 500$ ms. The sampling interval Δt for tracking control is set to 50 ms. The weighting matrices used are

$$\mathbf{Q} = \begin{bmatrix} \mathbf{Q}_p & \mathbf{0}_{9M \times 9N} \\ \mathbf{0}_{9N \times 9M} & \mathbf{Q}_a \end{bmatrix}, \quad \mathbf{R} = 0.05 \mathbf{I}_{9(M+N)-15},$$

where $\mathbf{Q}_p \in \mathbb{R}^{9M \times 9M}$ is a diagonal matrix of all zeros with 1000 as the non-zero entry at indices $(3M + 1)$ to $(3M + 6)$ and $(6M + 1)$ to $(6M + 6)$, and $\mathbf{Q}_a \in \mathbb{R}^{9N \times 9N}$ is a diagonal matrix of all zeros with 1 as the non-zero entry at indices 1 to 18. The rationale behind this state cost weighting is to prioritize penalizing the position and velocity from (1) in the lifted-space for deviation from the reference. We have used a low-order truncation with $M = 3$ and $N = 3$ for the lifted LTI model construction. Further, the attitude tracking error is defined as $\psi = \text{trace}(\mathbf{I}_3 - \mathbf{R}_{ref}^T \mathbf{R}) / 2$. The effectiveness of our Koopman-based formulation and LMPC is presented using three tracking tasks given below.

Following a helical path: the maneuver of the quadrotor following a helical path is demonstrated in Fig. 3(a) where $\mathbf{x}_{ref} = [t/20, \sin(t/6), 2 \cos(t/6)]^T$, $\mathbf{v}_{ref} = \dot{\mathbf{x}}_{ref}$, $\mathbf{R}_{ref} = \mathbf{I}_3$, and $\omega_{ref} = \mathbf{0}$; and initial conditions being $\mathbf{x}(0) = \mathbf{x}_{ref}(0)$, $\mathbf{v}(0) = \mathbf{v}_{ref}(0)$, $\mathbf{R}(0) = \mathbf{I}_3$, and $\omega(0) = \mathbf{0}$. The LMPC approach ensures that the quadrotor follows the helical path effectively by maintaining close alignment with the reference trajectory and velocity with time as seen in Fig. 3(b). Moreover, the quadrotor's attitude tracking error ψ is also of the order of 10^{-3} throughout the maneuver as seen in Fig. 3(c).

Following a Torus knot: The quadrotor's trajectory following a Torus knot is illustrated in Fig. 4(a) where $\mathbf{x}_{ref} = [\sin(0.1t) + 2 \sin(0.2t), \cos(0.1t) - 2 \cos(0.2t), -\sin(0.3t)]^T$, $\mathbf{v}_{ref} = \dot{\mathbf{x}}_{ref}$, $\mathbf{R}_{ref} = \mathbf{I}_3$, $\omega_{ref} = \mathbf{0}$; and initial conditions being $\mathbf{x}(0) = \mathbf{x}_{ref}(0)$, $\mathbf{v}(0) = \mathbf{v}_{ref}(0)$, $\mathbf{R}(0) = \mathbf{I}_3$, and $\omega(0) = \mathbf{0}$. The LMPC method effectively guides the quadrotor to adhere to the Torus knot path by closely matching the reference trajectory and

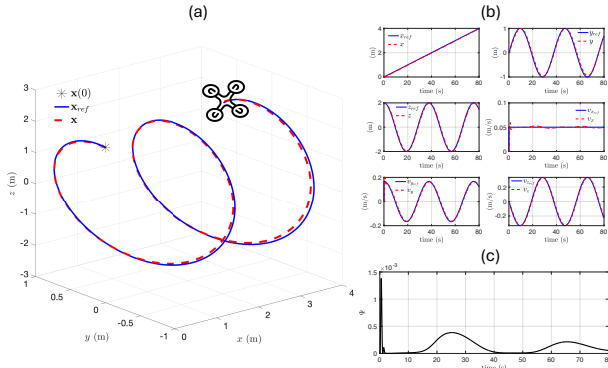


Fig. 3: Quadrotor following a helical path: (a) desired and actual trajectory, (b) position and velocities with time, (c) attitude error with time (animations on santoshraj कुमार.github.io/lcssgifs)

velocity over time, as demonstrated in Fig. 4(b). Additionally, the quadrotor’s attitude tracking error remains under 10^{-2} throughout the tracking of the path as illustrated in Fig. 4(c).

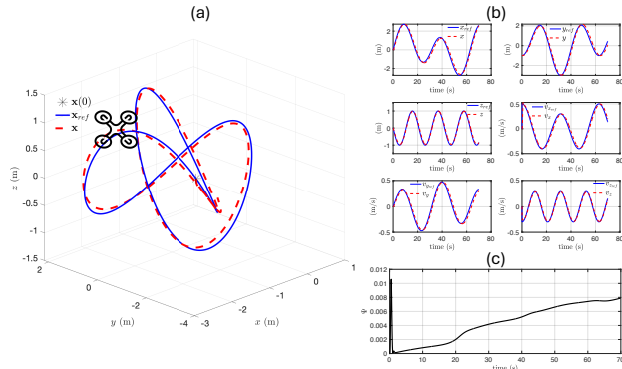


Fig. 4: Quadrotor following a Torus knot: (a) desired and actual trajectory, (b) position and velocities with time, (c) attitude error with time (animations on santoshraj कुमार.github.io/lcssgifs)

Hover task: The trajectory of the quadrotor moving to a desired position and hovering is demonstrated in Fig. 5(a) where $\mathbf{x}_{ref} = [1, 1.3, 2]^T$, $\mathbf{v}_{ref} = \mathbf{0}$, $\mathbf{R}_{ref} = \mathbf{I}_3$, and $\boldsymbol{\omega}_{ref} = \mathbf{0}$; and initial conditions being $\mathbf{x}(0) = \mathbf{0}$, $\mathbf{v}(0) = \mathbf{0}$, $\mathbf{R}(0) = \mathbf{I}_3$, and $\boldsymbol{\omega}(0) = \mathbf{0}$. The quadrotor achieves desired position and velocity in a time less than 20 sec as seen in Fig. 5(b), while maintaining an attitude error close to zero once the desired position is reached as depicted in 5(c).

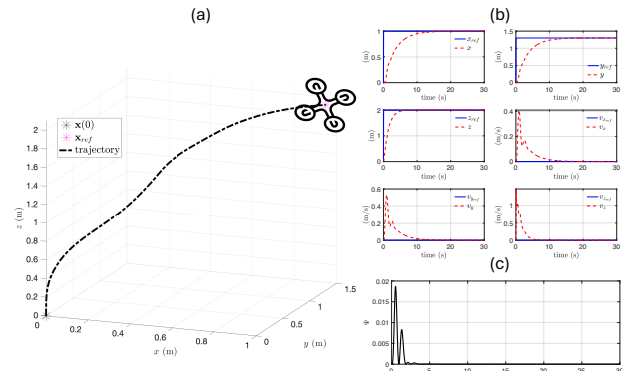


Fig. 5: Quadrotor performing a hover task: (a) trajectory with initial and reference point, (b) position and velocities with time, (c) attitude error with time (animations on santoshraj कुमार.github.io/lcssgifs)

The average solving time of the OCP (27) for the tasks in Figs. 3, 4, and 5 are 4.78 ms, 4.89 ms, and 4.91 ms, respectively. These results suggest that our Koopman-based LMPC has the potential for real-time hardware implementation.

V. CONCLUSION

This letter presented an analytical derivation of a Koopman-based countably infinite-dimensional linear embedding for nonlinear quadrotor dynamics on SE(3). Based on the linear embedding, a linear parameter-varying (LPV) control system is formulated with analytically justified truncation from the infinite-dimensional realization. The resultant LPV system is approximated as a linear time-invariant (LTI) system with virtual control inputs, preserving the controllability characteristics. Finally, the implementation of a linear model-predictive control (LMPC) scheme using the LTI system, as evidenced by numerical simulations, affirms its efficacy in addressing various tracking problems and highlights its potential for real-time application. Potential future work includes the formulation of constrained LMPC for the lifted dynamics and extension to fixed-wing UAVs.

REFERENCES

- [1] S. Sun, A. Romero, P. Foehn, E. Kaufmann, and D. Scaramuzza, “A comparative study of nonlinear mpc and differential-flatness-based control for quadrotor agile flight,” *IEEE Transactions on Robotics*, vol. 38, no. 6, pp. 3357–3373, 2022.
- [2] D. Mellinger, N. Michael, and V. Kumar, “Trajectory generation and control for precise aggressive maneuvers with quadrotors,” *The International Journal of Robotics Research*, vol. 31, no. 5, pp. 664–674, 2012.
- [3] G. Hoffmann, S. Waslander, and C. Tomlin, “Quadrotor helicopter trajectory tracking control,” in *AIAA guidance, navigation and control conference and exhibit*, 2008, p. 7410.
- [4] M. Budišić, R. Mohr, and I. Mezić, “Applied koopmanism,” *Chaos: An Interdisciplinary Journal of Nonlinear Science*, vol. 22, no. 4, 2012.
- [5] A. Mauroy and I. Mezić, “Global stability analysis using the eigenfunctions of the koopman operator,” *IEEE Transactions on Automatic Control*, vol. 61, no. 11, pp. 3356–3369, 2016.
- [6] A. Surana, “Koopman operator framework for time series modeling and analysis,” *Journal of Nonlinear Science*, vol. 30, no. 5, pp. 1973–2006, 2020.
- [7] S. L. Brunton, B. W. Brunton, J. L. Proctor, and J. N. Kutz, “Koopman invariant subspaces and finite linear representations of nonlinear dynamical systems for control,” *PLoS one*, vol. 11, no. 2, p. e0150171, 2016.
- [8] X. Ma, B. Huang, and U. Vaidya, “Optimal quadratic regulation of nonlinear system using koopman operator,” in *2019 American Control Conference (ACC)*. IEEE, 2019, pp. 4911–4916.
- [9] S. S. Narayanan, D. Tellez-Castro, S. Sutavani, and U. Vaidya, “Se (3) koopman-mpc: Data-driven learning and control of quadrotor uavs,” *IFAC-PapersOnLine*, vol. 56, no. 3, pp. 607–612, 2023.
- [10] Y. Kawahara, “Dynamic mode decomposition with reproducing kernels for koopman spectral analysis,” *Advances in neural information processing systems*, vol. 29, 2016.
- [11] B. Lusch, J. N. Kutz, and S. L. Brunton, “Deep learning for universal linear embeddings of nonlinear dynamics,” *Nature communications*, vol. 9, no. 1, p. 4950, 2018.
- [12] T. Chen and J. Shan, “Koopman-operator-based attitude dynamics and control on so(3),” *Journal of Guidance, Control, and Dynamics*, vol. 43, no. 11, pp. 2112–2126, 2020.
- [13] V. Zinage and E. Bakolas, “Koopman operator based modeling for quadrotor control on se (3),” *IEEE Control Systems Letters*, vol. 6, pp. 752–757, 2021.
- [14] T. Lee, M. Leok, and N. H. McClamroch, “Geometric tracking control of a quadrotor uav on se (3),” in *49th IEEE conference on decision and control (CDC)*. IEEE, 2010, pp. 5420–5425.
- [15] B. O. Koopman, “Hamiltonian systems and transformation in hilbert space,” *Proceedings of the National Academy of Sciences*, vol. 17, no. 5, pp. 315–318, 1931.
- [16] A. Surana, “Koopman operator based observer synthesis for control-affine nonlinear systems,” in *2016 IEEE 55th Conference on Decision and Control (CDC)*, 2016, pp. 6492–6499.
- [17] C.-T. Chen, *Linear system theory and design*. Saunders college publishing, 1984.
- [18] R. Verschuere, G. Frison, D. Kouzoupis, J. Frey, N. v. Duijkeren, A. Zanelli, B. Novoselnik, T. Albin, R. Quirynen, and M. Diehl, “acados—a modular open-source framework for fast embedded optimal control,” *Mathematical Programming Computation*, vol. 14, no. 1, pp. 147–183, 2022.